The Journal of Experimental Biology 205, 3891–3902 (2002)
Printed in Great Britain © The Company of Biologists Limited
JEB4521E

Two sniffing strategies in palinurid lobsters

J. A. Goldman* and S. N. Patek†

Biology Department, Duke University, Durham, NC 27708, USA

*Present address: American Institute of Biological Sciences, 1444 Eye Street, NW, Suite 200, Washington, DC 20005, USA
†Author for correspondence at present address: University of California, Department of Integrative Biology, Berkeley, CA 94720-3140, USA (e-mail: patek@socrates.berkeley.edu)
Authorship order was assigned arbitrarily

Accepted 23 September 2002

Summary

Most studies of lobster chemoreception have focused on the model systems of *Panulirus argus* (Palinuridae) and *Homarus americanus* (Nephropidae). We compare antennule morphology across lobsters and conduct the first kinematic study of antennule flicking in a palinurid species other than *P. argus*. High-speed video analysis shows that *Palinurus elephas* flicks at a rate more than an order of magnitude higher than in *P. argus*. However, both species flick their antennular flagella at a Reynolds number (*Re*) of approximately one, such that an asymmetry in the speed of the flick phases causes both species to have a leaky closing flick phase and a non-leaky opening phase. The antennular flagella of *P. argus* are nearly seven times longer than those of *P. elephas*, and, when compared across palinurid genera, *Panulirus* species sample far greater areas of water over greater spatial and time scales than do any other palinurid genera. Palinurid lobsters appear to have two sniffing strategies: low flick rates over a large area of water (e.g. *P. argus*) or high flick rates over a small area of water (e.g. *P. elephas*). *P. argus* is a highly informative model system in which to study aquatic chemoreception; however, its antennule anatomy and kinematics suggest a separate strategy, unique to *Panulirus* species, for sensing chemical plumes in fluid environments.

Key words: kinematics, olfaction, antennule, lobster, Palinuridae, chemoreception, *Panulirus argus*, *Palinurus elephas*, aesthetasc, leakiness, Reynolds number.

Introduction

Olfaction in a fluid environment can be regarded as a two-stage process in which fluid convection initially carries odor molecules to the region of a sensor and diffusion ultimately transports them to a receptor surface. Organisms have evolved different behavioral mechanisms to facilitate the convective stage of the process. For example, mammals sniff to transport scents over their olfactory surfaces. Snakes vibrate their tongues to move odors over their vomeronasal pouches (Halpern and Kubie, 1980). Male silkworm moths fan their wings to pass pheromones over their antennae (Loudon and Koehl, 2000). Fish flush water through olfactory organs (Døving et al., 1977; Kux et al., 1988). Malacostracan crustaceans, such as crabs, stomatopods and lobsters, flick their antennules to generate convective flows (Goldman and Koehl, 2001; Mead et al., 1999; Moore et al., 1991a; Schmitt and Ache, 1979; Snow, 1973).

Lobsters use their antennules to track the chemical signatures of food and conspecifics (Fig. 1A; Atema, 1995; Atema and Voigt, 1995; Derby and Atema, 1988; Derby et al., 2001; Ratchford and Eggleston, 1998; Reeder and Ache, 1980; Zimmer-Faust et al., 1985). The lateral flagellum of the antennule has rows of specialized chemosensory setae, the aesthetascs (Fig. 1B,C), in addition to other mechano- and chemosensory setae (Cate and Derby, 2001; Grünert and Ache, 1988; Laverack, 1964; Steullet et al., 2002). Lobsters ‘sniff’ by flicking the lateral flagellum through the water (Moore et al., 1991a; Schmitt and Ache, 1979); during the fast closing phase, water flows through the chemosensory aesthetascs, and during the slower opening phase, water is not replaced (Goldman and Koehl, 2001; Koehl et al., 2001). It has been suggested that the generation of such intermittent flows by antennules results in discrete sampling of the surrounding fluid (Moore et al., 1991a; Schmitt and Ache, 1979). Indeed, Koehl et al. (2001) showed empirically that antennule flicking allows spiny lobsters to take discrete samples of the temporal/spatial distribution of fine scale chemical plumes in the environment.

Lobsters locate odor sources by using their antennules to sample an odor plume’s structure (Atema, 1996; Moore and Atema, 1988, 1991; Moore et al., 1991b; Zimmer-Faust et al., 1995; reviewed in Weissburg, 2000; Atema, 1995). Within an odor plume, small filaments with high odor concentrations spread from the odor source. When crustaceans flick their antennules, they sample sharp concentration gradients of the plume filaments. By tracking the spatial and temporal

distribution of these filaments in the environment, as well as other environmental cues (e.g. current flow; Zimmer-Faust et al., 1995), they can localize the source of an odor.

The chemical and fluid characteristics that are processed by an organism are determined by the spacing of microscopic setae and a flagellum's speed during a flick (Koehl, 1995); these processes have been shown in both empirical and theoretical studies of cylinder arrays (Cheer and Koehl, 1987a,b; Hansen and Tiselius, 1992; Koehl, 1993, 1995, 1996, 2000; Loudon et al., 1994). In general, when fluid flows across a surface, the velocity of the fluid in contact with the surface is zero (no-slip condition); hence, a velocity gradient, also known as a boundary layer, develops in the region adjacent to the surface (Vogel, 1994). For a given geometry, the thickness of the boundary layer varies inversely with Reynolds number (*Re*) – a dimensionless parameter that describes the relative magnitude of inertial and viscous fluid forces in a given flow regime (Vogel, 1994). Fast, turbulent flows at large spatial scales are generally of high *Re*, whereas slow, laminar flows at small spatial scales are generally of low *Re*. The *Re* is defined as:

$$Re = UL/\nu , \quad (1)$$

where U is the freestream flow speed, L is a length scale, and ν is the kinematic viscosity of the fluid (Vogel, 1994).

The amount of fluid that passes through rather than around a lobster's aesthetasc array is determined by the array's leakiness. In an array of cylinders, when the boundary layers around two adjacent cylinders are large relative to the distance between them, some proportion of the incident fluid will be forced around rather than through the array. When the boundary layers are relatively small, more fluid will leak through the array. Thus, the leakiness of an array depends on (1) *Re*, which determines boundary layer thickness, and (2) the relative size of the gaps between adjacent cylinders, which is expressed as the ratio of the gap to the cylinder diameter (Koehl, 1995, 2000). Quantitatively, leakiness is the volume of fluid that flows through the gap between cylinders in an array divided by the volume of fluid that would flow through the same area had the cylinders been absent (Cheer and Koehl, 1987b).

Across species, changes in velocity and setal spacing can modify the transition point between leaky and non-leaky movements (Koehl, 1995). In a copepod, *Centropages furcatus*, the setae on the second maxillae are widely spaced and typically function as a rake (capturing particles as water flows through the structure). When maxillae velocity is decreased, the appendage acts like a paddle (most of the particle-laden water flows around rather than through the structure). By contrast, the copepod *Temora stylifera*, has more closely spaced setae and the maxillae normally function as paddles, but, when velocity is increased, the maxillae act as rakes. These different strategies illuminate the importance of both morphological and behavioral modifications for changing the fluid dynamics of sensory appendages across species (Koehl, 1995). An organism that modifies the speed of its sensory appendage and/or the relative size of the gaps between its sensory hairs can adjust the way it samples chemical information in the environment.

Studies of chemoreception in aquatic crustaceans have focused on a broad array of taxa, including spiny lobsters (Palinuridae: Derby and Atema, 1988; Grünert and Ache, 1988; Reeder and Ache, 1980), clawed lobsters (Nephropidae: Atema, 1995; Atema and Voigt, 1995), crayfish (Cambaridae: Dunham et al., 1997; Moore and Grills, 1999; Oh and Dunham, 1991) and crabs (Portunidae: Weissburg and Zimmer-Faust, 1993, 1994). Most studies of lobster chemoreception have focused on *Panulirus argus* (Palinuridae) and *Homarus americanus* (Nephropidae), with few studies comparing species within these families (Cate and Derby, 2002), although some studies have compared these model species to other crustaceans (e.g. Ghiradella et al., 1968; Laverack, 1985).

In the present study, we compare *Panulirus argus* (Caribbean spiny lobster) to *Palinurus elephas* (common spiny lobster) to determine how major structural differences in chemoreceptor organs influence the capture of odor molecules from the environment and to assess the relevance of the *P. argus* model to other palinurid lobsters. (Note: these species are in different genera with similar names.) We describe the morphology and kinematics of the antennular flagella in *P. elephas* through the use of scanning electron microscopy, high-speed videography and a new method of digital video analysis. We compare *Re* and leakiness parameters to those previously described in *P. argus* and propose a functional interpretation for the two dramatically different strategies used by these species in acquiring chemical information. We measure antennule structures across all major genera in the Palinuridae and estimate the amount of water sampled by different antennule sizes. To our knowledge, this is the first time that the antennular kinematics of a palinurid species other than *P. argus* has been studied. Furthermore, this comparative study offers a first step towards understanding the behavioral function of the remarkable antennule variation across the palinurid family.

Materials and methods

Animals

Palinurus elephas (Decapoda: Palinuridae) specimens were collected by Cleggan Lobster Fisheries Ltd (Galway, Ireland) and shipped to Duke University. They were housed in filtered, recirculating, synthetic seawater at 10–11°C in 227l glass aquaria.

Microscopy and morphological descriptions

The microscopic anatomy of the flagella was examined using stereo light microscopy and scanning electron microscopy (SEM). We removed the antennules from freshly euthanized lobsters. The tissue was immediately placed in 2% glutaraldehyde in phosphate-buffered saline and fixed for 1.5 h [see Dykstra (1992)]. The tissue was rinsed in distilled water

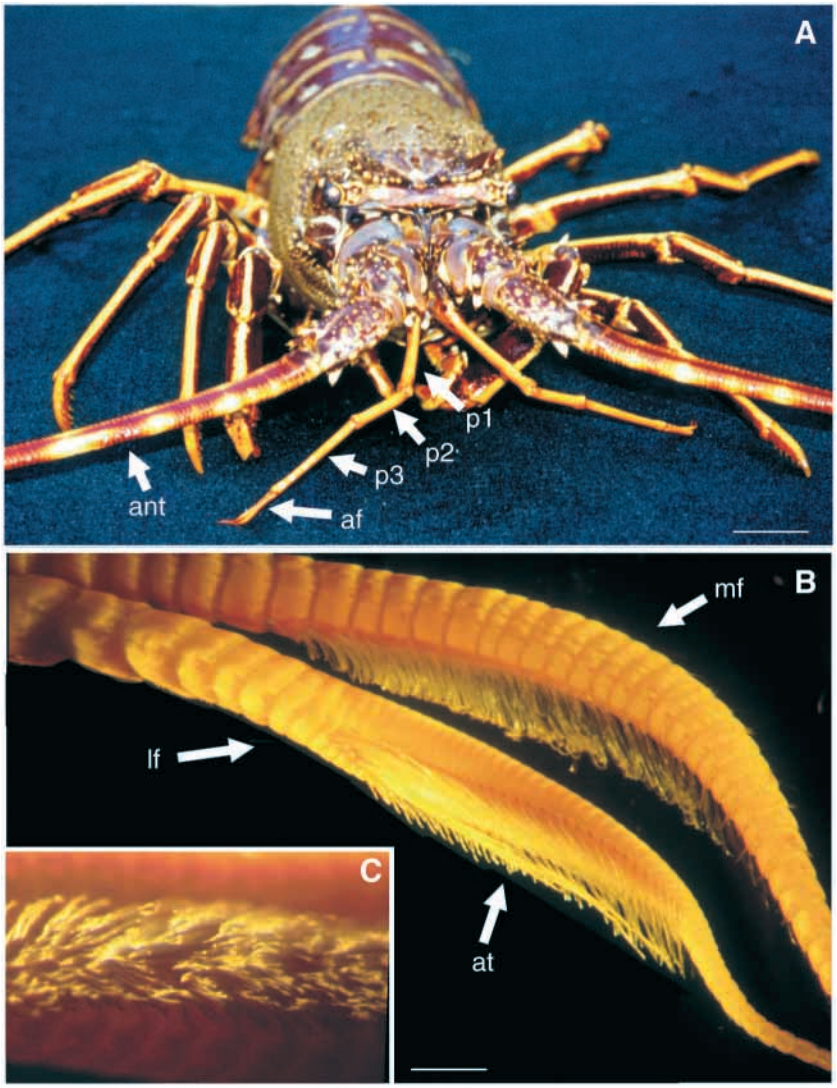

Fig. 1. The antennules and flagella of *Palinurus elephas*. (A) An anterior view of *P. elephas* (carapace length 138 mm) showing the location of the antennae (ant) and antennules. The antennules are composed of antennular peduncles with three segments (p1, p2 and p3) and antennular flagella (af). Scale bar, 26 mm. (B) The antennular flagella with the medial flagellum (mf) towards the top of the figure and the lateral flagellum (lf) below. Note the discrete aesthetasc tuft (at; length 8 mm) on the lateral flagellum. Scale bar, 1.7 mm. (C) An orthogonal view of the diffuse array of aesthetasc tips with the guard hairs removed.

and dehydrated in an ethanol series. The specimens were stored in 100% ethanol until critical point drying and then were sputter coated (60:40 gold:paladium mix, Anatech Hummer V, Anatech Ltd, Springfield, VA, USA) and observed at up to 2500× magnification with a scanning electron microscope (Philips 501 SEM, Oregon, USA). The lateral and medial flagella were cut into four and two smaller sections, respectively, in order to mount on stubs in the scanning electron microscope. The guard hairs were removed in some samples in order to view the aesthetascs.

Aesthetasc diameter and the gap distance between rows of aesthetascs were measured from digital images captured from the SEM (Scion Image, v.4.0.2, Maryland, USA). Aesthetasc diameter and gap distance between each aesthetasc were measured at the base of the aesthetascs near their insertion on the flagellum. Average measurement error was 2.3% of the mean. We sampled ten aesthetascs and ten gaps from four individuals. Digital SEM images of a calibration disk (Ted Pella, Inc., Redding, CA, USA) were used for calibrating images of antennules.

Comparative antennule morphology

We measured lengths of the peduncle segments and flagella of 17 lobster species using preserved specimens housed at the National Museum of Natural History, Smithsonian Institution, Washington, DC, USA. Each major genus of the Palinuridae was represented, as well as members of the Nephropidae (*Homarus americanus*) and the Scyllaridae (*Parribacus antarcticus*, *Scyllarus arctus*). Body size was approximated as carapace length (base of the rostrum to the posterior margin of the carapace). Two specimens per species were measured when possible.

High-speed videography

A high-speed video system (HR1000, Redlake Motionscope Systems, San Diego, CA, USA) recorded images of the *P. elephas* antennules as they flicked. The system's tripod-mounted camera recorded images of the two flagella on each antennule. Images of antennule flicking in which the lateral flagellum was perpendicular to the camera's lens were collected at 500 frames s^{-1} and stored on SVHS videotape. Later, video fields were digitized and stored as sequences of individual bitmap images (TIFF format).

Motion analysis

We designed an automated method that does not rely on traditional motion analysis techniques to track flagellum movement. Video images could not resolve natural markings on the flagella and we were unable to use physical markers because they either damaged the delicate antennules or were removed by the animal. To circumvent these problems, we quantified the motion of the antennule's lateral flagellum by tracking the intersection between the edge of the flagellum and a line fixed in the image plane (Fig. 2A). The line intersected the distal end of the aesthetasc-bearing region of the flagellum and ran tangent to the arc traced by a point on the flagellum when it moved. For the small angular excursions subtended by the flagella during a flick (approximately 5°), the maximum deviation between the

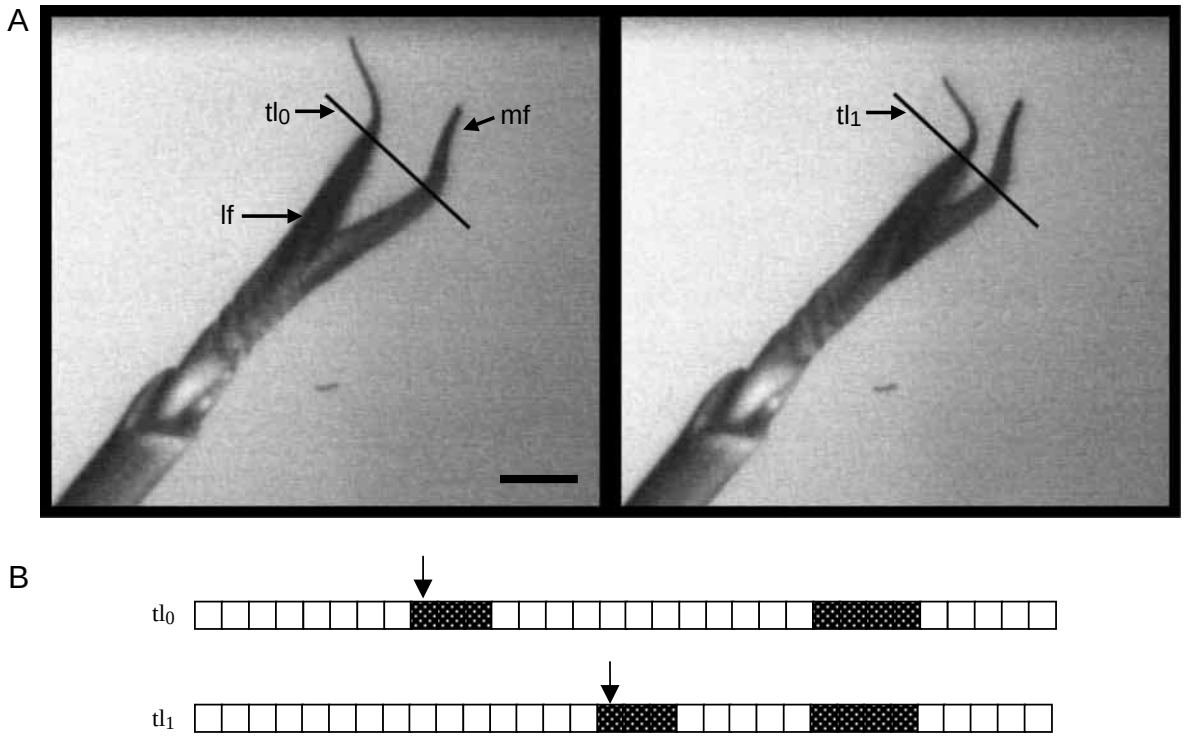

Fig. 2. Illustration of the video analysis technique used for tracking antennule movement. (A) Video images of a flicking right antennule show the motion of the lateral flagellum (lf) during the closing phase; the medial flagellum (mf) remains stationary. The location of the antennule edge was determined by superimposing a line tangent (tl) to the motion of the arc swept by the lateral flagellum. To clearly show the lateral flagellum's motion, this illustration presents images and tangent lines at the start (tl_0) and end (tl_1) of a 22 ms time period (images were actually sampled every 2 ms). Scale bar, 4.9 mm. (B) The pixel intensity profile from the tangent line (tl) was used to locate the lateral flagellum's edge and to calculate position and speed during a flick. For illustration purposes, we show a small number of pixels with an intensity profile including only white (background) or dark stippling (flagellum) rather than the hundreds of pixels and continuous shades of gray actually used in the analyses. Times tl_0 and tl_1 correspond to the tangent lines denoted as tl_0 and tl_1 in panel A. Arrows indicate the moving edge of the lateral flagellum.

tangent line and the circular path of a point on the flagellum was approximately 0.1% of the diameter and thus was neglected.

Image processing consisted of: (1) filtering, (2) sampling pixel intensity along the tangent line and (3) edge detection. First, an adaptive Wiener algorithm acted as a low-pass filter to reduce noise in the image [local means and standard deviations were calculated for each pixel using an area set at 5 pixel × 5 pixel window (Matlab v. 6, The Mathworks Inc., Natick, MA, USA)]. Second, a tangent line was drawn on the image for each flick sequence using a software graphical interface. Image-processing software sampled the intensity of each pixel along the line for each image in a sequence. Third, the edge was detected along the tangent line at locations where the intensity of the pixels changed from light (background) to dark (flagellum). We tracked the position of the intensity transition over the course of each flick (Fig. 2B).

We determined the position of the transition from background to flagellum by comparing the intensity difference between the end pixels of a 3-pixel wide window passed along the tangent line (Fig. 2). The position of the transition depended on a threshold value of intensity difference. Within a range of threshold values, our method detected the same edge but located it at slightly different positions. Outside of the threshold-value range, the method either detected an edge in the background (resulting from noise in the pixel intensity of the background) or did not detect an edge at all. Rather than choose a single threshold value arbitrarily, we determined a range of threshold values that properly detected all of the edges in a flick sequence and used the mean edge position determined over that range of threshold values. The standard deviation of edge position measurements over the range of threshold values never exceeded 3% of the mean.

To track the position of the flagellum over time we first filtered the raw position data to remove high-frequency noise and then calculated the speed. The filtering algorithm consisted of four steps: (1) filtering the data with a second-order low-pass Butterworth filter, (2) reversing, with respect to time, the output, (3) filtering with the same filter again and (4) reversing, with respect to time, the output of the second filter (Winter, 1990). Re-filtering of the reversed data introduced a phase shift equal and opposite to that introduced by the first filter, and thus the algorithm resulted in filtered data in phase with the raw data. Residual analysis revealed that a cutoff frequency of 100 Hz balanced the amount of noise passed through the filter with the amount of signal distortion introduced by the filter (Winter, 1990). We applied a numeric differentiation technique

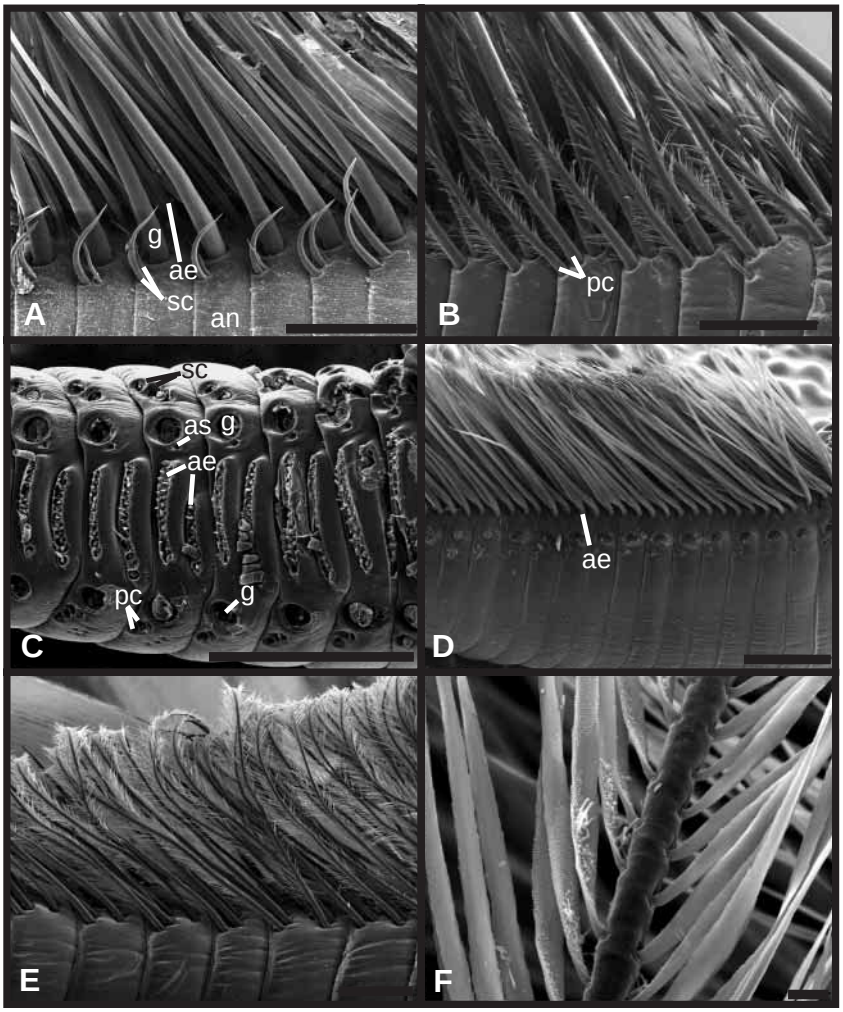

Fig. 3. Scanning electron micrographs of the setae found on the lateral and medial flagella of *Palinurus elephas*. The lateral flagellum (A–D) has an aesthetasc tuft, which is flicked through the water. The medial flagellum (E–F) remains stationary during the flick. Distal is towards the left of the page in images A–E. (A) The lateral region of the aesthetasc tuft shows the aesthetascs (ae), which form paired rows on each annulus (an) of the flagellum. A single guard hair (g) per annulus flanks both medial and lateral edges of the aesthetasc tuft. Paired simple companion hairs (sc) only are located on the lateral side of the aesthetasc tuft. Scale bar, 0.5 mm. (B) Paired plumose companion hairs (pc) are found only on the medial region of the aesthetasc tuft. Scale bar, 0.5 mm. (C) The ventro-lateral side of the lateral flagellum shows the positions of setae along the aesthetasc tuft. The asymmetric setae (as) are found on the lateral side of the aesthetasc tuft just proximal to the guard hairs (g). Scale bar, 0.5 mm. (D) The lateral region of the aesthetasc tuft is shown with guard hairs and companion hairs removed so that the paired arrangement of aesthetasc rows per annulus is visible. Scale bar, 0.5 mm. (E) Long plumose setae extend along the medial flagellum. Scale bar, 0.5 mm. (F) Each plumose hair on the medial flagellum has an array of setules extending along its axis. Scale bar, 0.01 mm.

to calculate the speed of the flagellum. The speed at a time point was estimated to be the distance moved by the flagellum divided by the time increment between two video frames.

We converted kinematic measurements from pixel units to SI units by measuring the pixel dimensions of a known antennule structure in the image using Scion Image (the actual size previously was measured on the live specimens). Imprecision, expressed as the standard deviation of repeated measures of the same structure, was typically 5% of the mean within an image and 3% of the mean between different images within a time sequence.

Determination of Reynolds number

In assigning the variables used to calculate *Re* (equation 1), we recognized that to an observer fixed in still fluid during a flick, the flagellum's speed equals the freestream flow speed in the flagellum's reference frame. Thus, we followed convention and chose *U* as either the peak or mean speed of the lateral flagellum during each phase of a flick (Goldman and Koehl, 2001; Mead et al., 1999). Because a flicking flagellum rotates about a fixed point, the freestream flow, and thus *Re*, will vary linearly along the flagellum's length. We report speeds and *Re* values encountered at the distal end of the aesthetasc-bearing region of the antennule. Aesthetasc diameter is used as the length scale (*L*) to be consistent with both empirical studies of flow through arrays of cylinders and studies of other biological sensors that bear hair-like sensilla (Goldman and Koehl, 2001; Hansen and Tiselius, 1992; Koehl, 1993, 1996, 2000; Mead et al., 1999). The kinematic viscosity (ν) of seawater (35‰) at 10°C is $1.36\times10^{-6}\,m^2\,s^{-1}$ (Sverdrup et al., 1942; Vogel, 1994).

Statistics

We tested whether the following kinematics parameters varied between the closing and opening phases of each flick: *Re*, maximum and average flagellum speed, duration and distance moved (excursion). For duration measurements, 26–39 flicks from each of four individuals were measured. For all other kinematic measurements, 11–39 flicks from each of four individuals were measured. Data were tested for normality using a Shapiro–Wilk test (Zar, 1999). As the data did not conform to a normal distribution, differences between flick phases across individuals were tested using a nonparametric Kruskal–Wallis test (Zar, 1999). Significance level was set at P=0.01 to account for multiple comparisons (Sokal and Rohlf, 1981).

Table 1. *Lengths of antennule structures*

Antennule structures*	Mean size (±S.D.)†
Carapace length	144 (4.9) mm
1st peduncular segment (p1)	56.7 (7.9) mm
2nd peduncular segment (p2)	22.9 (3.9) mm
3rd peduncular segment (p3)	37.9 (5.2) mm
Medial flagellum (mf)	29.9 (4.9) mm
Lateral flagellum (lf)	25.6 (3.1) mm
Aesthetasc diameter	26.1 (0.7) μm
Gap width	84.0 (11.6) μm
Gap:diameter	3.2

*Letters correspond to the labels in Fig. 1.
†Measurements are taken from four individuals.

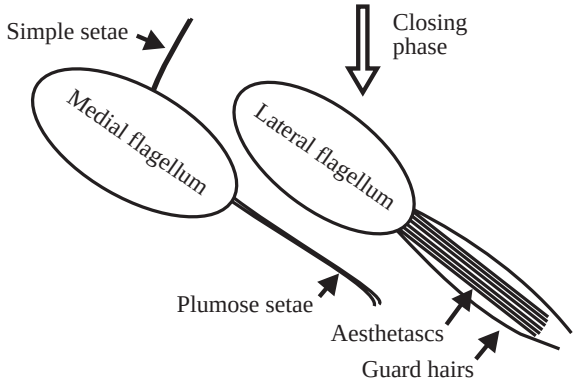

Fig. 4. A cross-sectional view of the antennule flagella and setae during a flick. The lateral flagellum is rapidly flicked ventrally during the closing phase (towards the bottom of the figure) and opened more slowly. Aesthetascs are aligned such that fluid flows between rows. The medial flagellum is not actively moved and its plumose setae remain slightly below the lateral flagellum during the flicks. The location of the medial flagellum's simple setae shifts medio-laterally along the length of the flagellum.

Results

Morphology

On the lateral flagellum of *Palinurus elephas*, the ventro-laterally projecting aesthetascs form paired rows on each annulus of the distal half of the flagellum (Fig. 3). The tips of the aesthetascs form a diffuse cluster, which lacks the zigzag pattern described in *Panulirus argus* (Fig. 1C; Goldman and Koehl, 2001). The number of aesthetascs per row decreases as the flagellum tapers to a thin, flexible point. Dimensions of the aesthetascs and their spacing on the flagellum are listed in Table 1. Asymmetric setae are found on each annulus immediately adjacent to the medial edge of the aesthetasc rows (Fig. 3C). Dwarfing these setae are guard setae that flank each pair of aesthetasc rows and form a canopy over the aesthetascs (Fig. 3A). Guard hairs on the lateral side of the aesthetasc tuft are plumose. Outside the guard hairs are pairs of companion setae (Cate and Derby, 2001; Fig. 3A–C). The companion setae found on the lateral side of the aesthetasc rows are simple (Fig. 3A); however, the companion setae on the medial side are plumose (Fig. 3B) [similar to the pattern found in the Red rock lobster, *Jasus edwarsii* (Cate and Derby, 2002)].

An array of plumose setae extends along the length of the medial flagellum (Fig. 3E,F). These setae extend ventro-

Table 2. *Length of peduncle segments and flagella divided by carapace length across 17 lobster species*

Genus	Species	Carapace lengths (mm)*	1st segment	2nd segment	3rd segment	Medial flagellum	Lateral flagellum
Jasus	*edwarsii*	77, 87	0.40	0.20	0.27	0.17	0.14
Jasus	*verreauxi*	80, 83	0.31	0.11	0.16	0.13	0.11
Justitia	*longimanus*	29, 44	0.71	0.30	0.32	0.29	0.20
Linuparus	*trigonus*	81, 94	0.29	0.11	0.15	0.15	0.13
Palinurus	*elephas*	138, 145, 147, 148	0.40	0.16	0.27	0.21	0.18
Panulirus	*argus*	61, 81	0.53	0.23	0.20	1.41	1.21
Panulirus	*homarus*	41	0.42	0.26	0.19	2.19	1.41
Panulirus	*inflatus*	37	0.39	0.23	0.21	1.67	1.13
Panulirus	*japonicus*	46, 51	0.56	0.22	0.23	1.42	1.25
Panulirus	*penicillatus*	75, 93	0.36	0.17	0.18	0.97	0.75
Panulirus	*versicolor*	50	0.55	0.30	0.29	3.14	2.01
Projasus	*bahamondei*	58, 52	0.51	0.18	0.37	0.24	0.16
Puerulus	*angulatus*	45, 49	0.50	0.15	0.21	0.39	0.33
Palinurellus	*weineckii*	56	0.27	0.13	0.12	0.18	0.13
Homarus	*americanus*	67, 62	0.12	0.04	0.04	0.53	0.44
Parribacus	*antarcticus*	30, 33	0.17	0.25	0.18	0.14	0.11
Scyllarus	*arctus*	95, 86	0.17	0.20	0.21	0.09	0.07

*The number of carapace length measurements indicates the number of specimens measured.
Homarus americanus (Nephropidae), *Parribacus antarcticus* (Scyllaridae) and *Scyllarus arctus* (Scyllaridae) are included as outgroup comparisons.

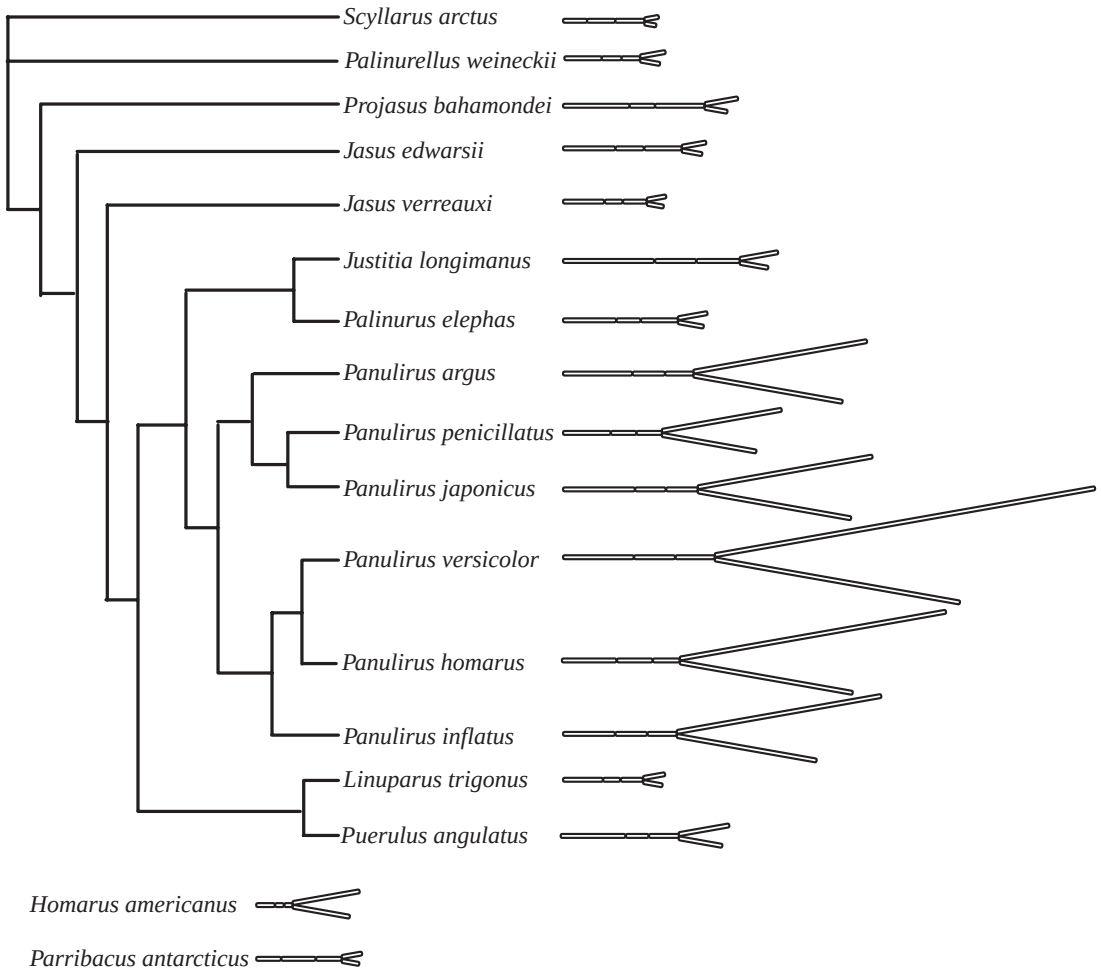

Fig. 5. Schematics of relative antennule lengths mapped onto a palinurid phylogeny. Medial flagellum is towards the top of the figure. The antennule lengths were divided by body size to show proportional differences across taxa. The phylogeny is modified from a morphological phylogeny (S. N. Patek and T. H. Oakley, submitted). The phylogenetic relationships of the Palinuridae have proved difficult to resolve, possibly due to fast radiations over ancient time scales (Patek, 2001); morphological and molecular rDNA sequence data have not consistently resolved genus-level relationships (Baisre, 1994; Patek, 2001; S. N. Patek and T. H. Oakley, submitted). *Homarus americanus* (Nephropidae), *Scyllarus arctus* (Scyllaridae) and *Parribacus antarcticus* (Scyllaridae) are included for outgroup comparisons.

laterally and remain ventral to the lateral flagellum during a flick (Fig. 4). An array of long, simple setae extends along the dorsal surface of the flagellum (Fig. 4). The long axis of the simple setae extends dorso-ventrally, whereas the plumose setae run perpendicular to the lateral flagellum's flick (Figs 3, 4).

Panulirus species have considerably longer flagella per body length than any other measured species, with the medial flagellum extending to up to three times the carapace length (Table 2; Fig. 5). The medial flagellum is longer than the lateral flagellum in all the species. The total peduncle length is relatively constant across taxa, although *Justitia longimanus* (West Indian furrow lobster) has a relatively high total peduncle length. Excepting *Parribacus* spp. and *Scyllarus* spp., the first segment of the peduncle is longer than the subsequent segments (Fig. 5; Table 2). The second and third segments of the peduncle are similar to each other in length. Lateral flagellum length varies dramatically across the lobsters (Fig. 6A). By contrast, most variation in total peduncle length appears to be explained by body size across taxa (Fig. 6B; Table 2).

Kinematics and Reynolds number

The flick of the lateral flagellum of a *P. elephas* antennule is a short reciprocal motion during which the flagellum executes a ventral excursion (closing phase) followed by an immediate return to or near the initiation point (opening phase) (Fig. 4). The medial flagellum is not actively moved during a flick but it does flex slightly in passive response to the impulsive motion of the lateral flagellum. Flicks were often executed in rapid succession with interspersed periods of quiescence (Fig. 7).

We found significant differences between flick phases in all measured parameters except excursion distance

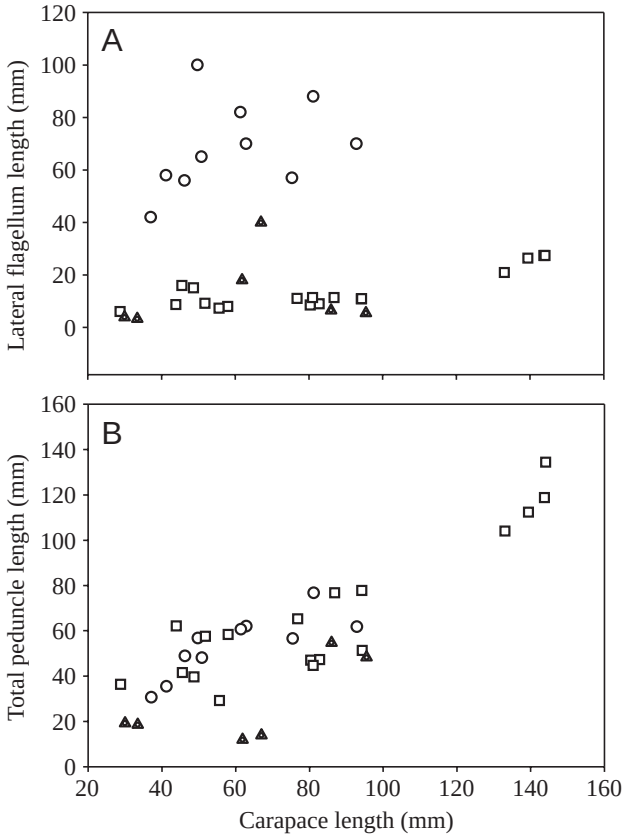

Fig. 6. Comparisons of lateral flagellum length (A) and peduncle length (B) for a given body size (carapace length) across lobster species. Circles represent individuals from the *Panulirus* genus. Squares represent members of the Palinuridae other than *Panulirus*. Triangles represent members of the Scyllaridae and Nephropidae.

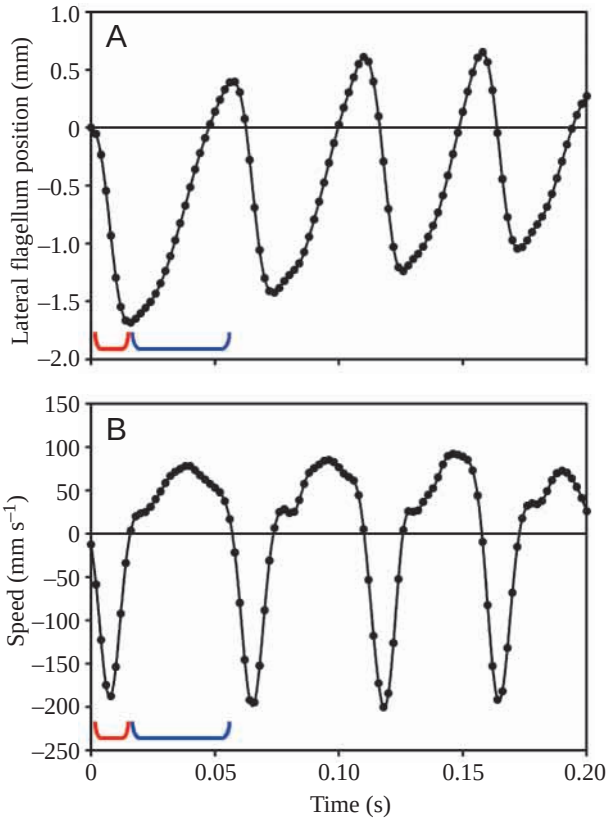

Fig. 7. Kinematic chronology of four representative flicks produced by a *Palinurus elephas* individual. (A) The lateral flagellum is shown at the starting position (arbitrarily set as zero) in which it is opened at a maximum distance from the medial flagellum. Then, the flagellum rapidly closes (red bracket) and slowly opens (blue bracket) four times. (B) The closing phase (red bracket, negative speed values) is faster and of shorter duration than the opening phase (blue bracket, positive speed values) of each flick.

(Table 3). Individuals differed significantly ($P \ll 0.01$, $N=4$) in all parameters except flick duration, so flick phase comparisons were calculated within each individual. Both the peak and the mean speed of the initial closing phase were approximately twice those of the opening phase of the flick (Fig. 7; Table 3). Furthermore, as the distance traveled by the flagellum was nearly equal in both phases of the flick, the duration of the flick phases also differed by a factor of approximately two (Fig. 7; Table 3). The *Re* of an aesthetasc during both phases of a flick is in the order of one. During the closing phase, the aesthetasc *Re* is approximately twice the aesthetasc *Re* during the opening phase (Table 3).

Discussion

Palinurus elephas and *Panulirus argus* have strikingly different antennule structures and kinematics yet, in spite of these differences, both species sample the fluid environment in a fundamentally similar way. We begin by discussing our findings in *P. elephas* and compare them with published studies of *P. argus*. Second, we make a broader comparison across palinurid genera and consider how the two flicking strategies in these species could influence the acquisition of spatial and temporal information contained in odor plumes.

Flicking kinematics and morphology in Palinurus elephas *and* Panulirus argus

P. elephas sniffs by flushing more water through the aesthetasc array during the relatively rapid closing phase of each flick than during the slower opening phase. By flicking its lateral flagella such that the aesthetasc tuft operates at *Re* values of approximately one, the leakiness of the aesthetasc array is sensitive to small changes in *Re*. If the aesthetasc array operated in an *Re* range that was an order of magnitude higher or lower, small *Re* changes would not affect leakiness: at *Re* values of approximately one, small differences in the speed of flick phases cause relatively dramatic differences in the leakiness of the aesthetasc array. If we apply the leakiness estimates generated by Hansen and Tiselius (1992; pp. 826-827) to the present study, we find that the leakiness of *P. elephas* aesthetasc arrays averages approximately 0.40 (0.70 peak) during the closing phase and 0.25 (0.30 peak) during the opening phase of

Table 3. *Comparison of kinematic and flow parameters during the two phases of the flick of* Palinurus elephas

Kinematic parameters	Closing phase (mean ± S.D.)*	Opening phase (mean ± S.D.)*	Average χ^2
Peak speed (mm s^{-1})	158 (73)	73 (33)	33.1**
Mean speed (mm s^{-1})	88 (42)	45 (20)	30.2**
Duration (s)	0.018 (0.002)	0.037 (0.003)	37.0**
Excursion (mm)	1.56 (0.67)	1.61 (0.69)	0.465
Re (based on peak speed)	3.1 (1.4)	1.4 (0.6)	33.1**
Re (based on mean speed)	1.7 (0.8)	0.9 (0.4)	30.2**

*Mean values across four individuals.

Average Chi-square (χ^2) values indicate for each parameter whether closing and opening phases were statistically significantly different. ** indicates $P \ll 0.01$.

Table 4. *Comparison of functionally important flick parameters in two palinurid species*

Flick parameters	*Palinurus elephas*[a]	*Panulirus argus*
Lateral flagellum length divided by carapace length	0.18 (0.02)	1.21 (0.18)[a]
Aesthetasc diameter (μm)	26.1 (0.7)	22[b]
Gap:diameter	3.2	5.4[b]
Excursion (mm)	1.56 (0.67)	7[c]
Mean *Re* closing phase	1.7 (0.8)	1.7[b,d]
Mean *Re* opening phase	0.9 (0.4)	0.5[b,d]
Mean speed closing phase (mm s^{-1})	88 (42)	72[b,d]
Mean speed opening phase (mm s^{-1})	46 (20)	24[b,d]
Duration closing phase (s)	0.018 (0.002)	0.10[e]
Duration opening phase (s)	0.037 (0.003)	0.34[e]
Kinematic viscosity (10^{-6} m^2 s^{-1})	1.36[f]	0.94[g]

[a]Data from the present study. Values for *Palinurus elephas* are means (± S.D.) of four individuals.

[b]Data from Goldman and Koehl (2001).

[c]Calculated as the mean speed of the closing phase multiplied by the duration of the closing phase.

[d]Converted to represent the distal end of the lateral antennular flagellum rather than the mid-point of the aesthetasc array by assuming that the aesthetasc array occupies the distal third of the flagellum and that speed varies linearly along its length.

[e]J. A. Goldman, unpublished data.

[f]At 10°C; data from Sverdrup et al. (1942) and Vogel (1994).

[g]At 25°C; data from Sverdrup et al. (1942) and Vogel (1994).

flicks. Hence, *P. elephas* sniffs by varying the flagellum's speed between the two flick phases, such that the closing phase is 60–130% more leaky than the opening phase.

Considering that mammals, snakes and other crustaceans discretely sample odors, it comes as no particular surprise that *P. elephas* also does so. It is surprising, however, that none of the factors that determine *Re* – flow speed, aesthetasc diameter and kinematic viscosity – are the same in *P. elephas* and *P. argus*, yet the mean *Re* of the closing phase is the same in each species and the mean *Re* of the opening phase is remarkably similar (Table 4). Both species operate their antennules in the *Re* range where leakiness is sensitive to the speed of the flick. If the flagella of *P. elephas* were merely geometrically scaled up to be the same length as those of *P. argus* and the angular velocity held constant, the relative spacing of the aesthetascs would remain constant but the *Re* range would cause both phases of the flick to be very leaky and the animal could not take discrete odor samples. On the other hand, if the flagella of *P. argus* were simply scaled down to the same length as *P. elephas*, neither flick phase would allow much fluid to enter the aesthetasc array and diffusion would move molecules from the fluid to the surface of the sensilla [although see Trapido-Rosenthal et al. (1987) for a discussion of enzyme-mediated chemoreception at sensillar surfaces]. Thus, in spite of both morphological and kinematic differences, *P. elephas* and *P. argus* discretely sample the fluid by flushing it through their aesthetasc arrays during the fast, leaky closing phase of a flick and retaining that sample of fluid during the slower, less leaky opening phase (Koehl, 2000; Goldman and Koehl, 2001; Koehl et al., 2001).

Even though *P. elephas* and *P. argus* use the same mechanism to discretely sample odors, the spatial and temporal characteristics of the water samples are distinctly different. The duration of each flick phase is nearly an order of magnitude lower in *P. elephas* than in *P. argus* (Table 4), hence the two species have vastly different flicking frequencies. *P. argus* flick at a frequency between 0.4 Hz and 1.5 Hz and increase flicking rates up to 3.5 Hz in the presence of food scent (Gleeson et al., 1993; Goldman and Koehl, 2001). We found that *P. elephas* flick at approximately 20 Hz; in one case this rate was sustained for over 0.8 s. In addition, the lateral flagella of *P. argus* are nearly seven times longer and the distal end of each flagellum travels four to five times further during a flick than do the lateral flagella of *P. elephas* (Tables 3, 4; Figs 5, 6).

Differences in the setae on the medial and lateral flagella also distinguish *P. elephas* and *P. argus*. Non-aesthetasc setae are important in acquiring mechanical and chemical information, complementary to that acquired with the aesthetascs (Steullet et al., 2001). On the lateral flagellum, *P. argus* has simple companion setae, whereas *P. elephas* and other palinurids have plumose companion setae (pc, Fig. 3; Cate and Derby, 2001, 2002). The function of these companion setae has yet to be determined, but the absence/loss of setules in *Panulirus* species suggests a change in mechanical sensitivity through modification of flow around the setae. On the medial flagellum, the plumose setae of *P. elephas* appear as though they would influence flow into the aesthetasc array during the closing phase of the flick (Fig. 4), but, at these *Re* values, motion near surfaces does not alter the leakiness of cylinder arrays (Loudon et al., 1994). *P. elephas* lacks the peculiar zigzag orientation of aesthetasc tips found in *P. argus*, which has been proposed to channel fluid between neighboring aesthetascs and thereby facilitate diffusion across the laminar region surrounding aesthetascs (Fig. 1C; Gleeson et al., 1993; Goldman and Koehl, 2001). In *P. argus*, fixation of the antennules can disrupt the zigzag arrangement of the aesthetasc

tips; thus, the clustering of aesthetasc tips towards the center of rows in *P. elephas* may be an artifact of the glutaraldehyde and alcohol tissue preservation applied to the flagella.

Antennule morphology across the Palinuridae

Both antennular flagellum length and total peduncle length vary across the Palinuridae (Table 2; Figs 5, 6). Peduncle length is relatively short in the nephropid lobsters, however most variability across the palinurids can be explained by body size (Figs 5, 6). Antennular flagellum length, by contrast, is highly variable across the palinurids.

While the peduncle length determines the maximum distance from the animal at which water can be sampled, the flagellum length determines the amount of water sampled per flick (proportional to the number of aesthetasc rows on the tuft). In each species, we estimated the area of water sampled per degree of movement (Δ) by the lateral flagellum as follows:

$$\Delta = \pi(\lambda^2 - (0.6\lambda)^2)/360\,, \quad (2)$$

which simplifies to

$$\Delta = 0.0056\lambda^2\,, \quad (3)$$

where λ is the lateral flagellum length. In *P. elephas*, the aesthetasc rows cover, on average, 0.37λ, whereas in *P. argus* the array extends approximately 0.5λ (Cate and Derby, 2001). Hence, we conservatively estimated that the aesthetasc rows extended the distal 0.4 proportion of λ. Δ is dramatically variable across taxa (Fig. 8). In the *Panulirus* genus [considered monophyletic (McWilliam, 1995; S. N. Patek and T. H. Oakley, submitted; Ptacek et al., 2001)], Δ is 1–2 orders of magnitude greater than in the other lobster taxa; effects of body size are barely visible at this level of comparison (Figs 6, 8).

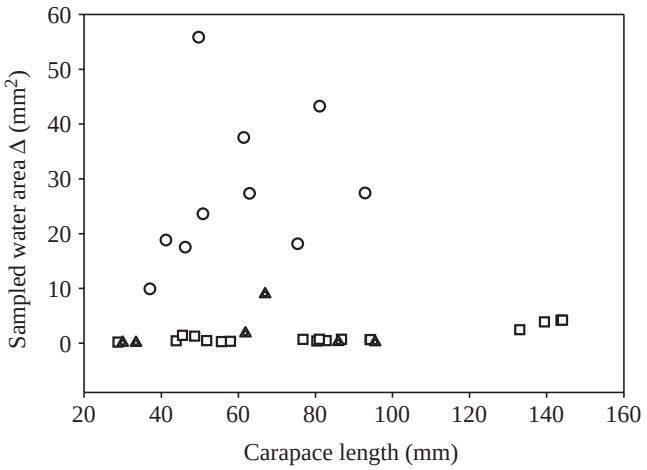

Fig. 8. Sampled water area (Δ) varies dramatically with small increments in lateral flagellum length. *Panulirus* species (circles) sample orders of magnitude larger water area per one degree of a closing phase than do other palinurid species (squares) and nephropid and scyllarid lobsters (triangles).

Two flicking strategies in palinurid lobsters

Flicking antennules collect both spatial and temporal information about a plume's structure (reviewed in Crimaldi et al., 2002; Weissburg, 2000). Models by Crimaldi et al. (2002) show that flicking (1) increases the number of concentration peaks (plume filaments) sampled per unit time, (2) increases the probability of sampling a high concentration plume filament and (3) permits two-dimensional sampling of the spatial structure of the plume. The fast response and integration times of both *Homarus americanus* (Nephropidae) and *Panulirus argus* (Palinuridae) receptor cells suggest that information about odor concentration and filament encounter can be acquired during and across flicks (Fadool et al., 1993; Gomez and Atema, 1996a,b; Gomez et al., 1994a,b, 1999; Moore and Atema, 1988; Schmiedel-Jakob et al., 1989).

P. argus, with its long antennules and slow flick rates, and *P. elephas*, with its short antennules and fast flick rates, use two different flicking strategies to sample the environment. Higher flick rates permit *P. elephas* to acquire shorter temporal samples of the environment than *P. argus* and, up to the temporal limits of the sensory receptors, can resolve shorter temporal fluctuations of filament concentrations as they move relative to the animal. Shorter antennules permit *P. elephas* to sample smaller areas of the plume than *P. argus* (Fig. 8) and can potentially resolve smaller spatial scale variations in plume filaments. *P. argus* samples a larger area of the plume per flick, which increases the probability of encountering an odor filament, but at the expense of small scale spatial resolution of the plume. By contrast, *P. elephas* samples small areas of water over shorter time scales and thus has higher spatial resolution of the plume compared with *P. argus*. However, if we take into account both (1) the probability of encountering an odor filament in the sampled area of a flick (high in *P. argus* and low in *P. elephas*) and (2) the probability of odor encounter based on the rate of flicking (low in *P. argus* and high in *P. elephas*), it remains to be determined whether these two species actually differ in the probability of encountering odor filaments.

Clearly, many factors influence evolutionary diversification of antennules in spiny lobsters. Spiny lobsters inhabit a wide range of habitats, from shallow reefs to deep-sea mud flats (George and Main, 1967; Holthuis, 1991; Kanciruk, 1980; Lozano-Alvarez and Biornes-Fourzan, 2001; Sharp et al., 1997), and exhibit a range of social behaviors across species and in the course of development (Childress and Herrnkind, 1996; Phillips et al., 1980). Odors play a central role in social behavior, and detection is limited by concentration (Childress and Herrnkind, 2001; Ratchford and Eggleston, 1998). While little is known of social and food searching behavior in *P. elephas* (Hunter, 1999), other spiny lobsters have been shown to rely on odor to locate food (Zimmer-Faust and Case, 1983; Zimmer-Faust et al., 1985), with *Panulirus* species foraging exceptionally long distances compared with other palinurids (Butler et al., 1999; MacDiarmid et al., 1991). The interplay between fluid dynamics, size, habitat and behavior is complex but critical to informing our understanding of evolutionary

changes in antennule morphology. Perhaps the most fundamental conclusion to be drawn from the present study is that, with their extraordinarily long flagella, *Panulirus* is the unusual genus in palinurid lobsters. While *P. argus* continues to be an informative model system, the next step is to examine the evolutionary history and current function of these two palinurid flicking strategies.

D. Schmitt and the Duke University Animal Locomotion laboratory (NSF No. SBR-9904-401) generously loaned their high-speed video system. We thank M. Koehl and K. Mead for valuable discussions. J. Birch, N. Danos, M. McHenry and D. Simon provided assistance with data analysis and implementation. We thank L. Eibest and the Duke University Scanning Electron Microscopy laboratory. This manuscript benefited from the comments of two anonymous reviewers. Funding was provided to S. N. P. by the Miller Institute for Basic Research in Science and the National Science Foundation DIG No. 9972597.

References

Atema, J. (1995). Chemical signals in the marine environment: Dispersal, detection, and temporal signal analysis. *Proc. Natl. Acad. Sci. USA* **92**, 62-66.

Atema, J. (1996). Eddy chemotaxis and odor landscapes: exploration of nature with animal sensors. *Biol. Bull.* **191**, 129-138.

Atema, J. and Voigt, R. (1995). Behavior and sensory biology. In *Biology of the Lobster Homarus americanus* (ed. J. Factor), pp. 313-348. New York: Academic Press.

Baisre, J. A. (1994). Phyllosoma larvae and the phylogeny of the Palinuroidea (Crustacea: Decapoda): a review. *Aust. J. Mar. Fresh. Res.* **45**, 925-944.

Butler, M. J., IV, MacDiarmid, A. B. and Booth, J. D. (1999). The cause and consequence of ontogenetic changes in social aggregation in New Zealand spiny lobsters. *Mar. Ecol. Prog. Ser.* **188**, 179-191.

Cate, H. S. and Derby, C. D. (2001). Morphology and distribution of setae on the antennules of the Caribbean spiny lobster *Panulirus argus* reveal new types of bimodal chemo-mechanosensilla. *Cell Tissue Res.* **304**, 439-454.

Cate, H. S. and Derby, C. D. (2002). Hooded sensilla homologues: structural variations of a widely distributed bimodal chemomechanosensillum. *J. Comp. Neurol.* **444**, 435-357.

Cheer, A. Y. L. and Koehl, M. A. R. (1987a). Fluid flow through filtering appendages of insects. *IMA J. Math. App. Med. Biol.* **4**, 185-199.

Cheer, A. Y. L. and Koehl, M. A. R. (1987b). Paddles and rakes: fluid flow through bristled appendages of small organisms. *J. Theor. Biol.* **129**, 17-39.

Childress, M. J. and Herrnkind, W. F. (1996). The ontogeny of social behaviour among juvenile Caribbean spiny lobsters. *Anim. Behav.* **51**, 675-687.

Childress, M. J. and Herrnkind, W. F. (2001). The guide effect influence on the gregariousness of juvenile Caribbean spiny lobsters. *Anim. Behav.* **62**, 465-472.

Crimaldi, J. P., Koehl, M. A. R. and Koseff, J. R. (2002). Effects of the resolution and kinematics of olfactory appendages on the interception of chemical signals in a turbulent odor plume. *Environ. Fluid Mech.* **2**, 35-63.

Derby, C. and Atema, J. (1988). Chemoreceptor cells in aquatic invertebrates: peripheral mechanisms of chemical signal processing in decapod crustaceans. In *Sensory Biology of Aquatic Animals* (ed. J. Atema, R. Fay, A. Popper and W. Tavolga). pp. 365-385. New York: Springer-Verlag.

Derby, C. D., Steullet, P., Horner, A. and Cate, H. (2001). The sensory basis of feeding behaviour in the Caribbean spiny lobster, *Panulirus argus*. *Mar. Fresh. Res.* **52**, 1339-1350.

Døving, K. B., Dubois-Dauphin, M., Holley, A. and Jourdan, F. (1977). Functional anatomy of the olfactory organ of fish and the ciliary mechanism of water transport. *Acta Zool. (Stock)* **58**, 245-255.

Dunham, D. W., Ciruna, K. A. and Harvey, H. H. (1997). Chemosensory role of antennules in the behavioral integration of feeding by the crayfish *Cambarus bartonii*. *J. Crust. Biol.* **171**, 27-32.

Dykstra, M. J. (1992). Biological Electron Microscopy: Theory, Techniques, and Troubleshooting. New York: Plenum Press.

Fadool, D. A., Michel, W. C. and Ache, B. W. (1993). Odor sensitivity of cultured lobster olfactory receptor neurons is not dependent on process formation. *J. Exp. Biol.* **174**, 215-233.

George, R. W. and Main, A. R. (1967). The evolution of spiny lobsters (Palinuridae): a study of evolution in the marine environment. *Evolution* **21**, 803-820.

Ghiradella, H. T., Case, J. F. and Cronshaw, J. (1968). Structure of aesthetascs in selected marine and terrestrial decapods: chemoreceptor morphology and environment. *Am. Zool.* **8**, 603-621.

Gleeson, R. A., Carr, W. E. S. and Trapido-Rosenthal, H. G. (1993). Morphological characteristics facilitate stimulus access and removal in the olfactory organ of the spiny lobster, *Panulirus argus*: insight from the design. *Chem. Senses* **18**, 67-75.

Goldman, J. A. and Koehl, M. A. R. (2001). Fluid dynamic design of lobster olfactory organs: high speed kinematic analysis of antennule flicking by *Panulirus argus*. *Chem. Senses* **26**, 385-398.

Gomez, G. and Atema, J. (1996a). Temporal resolution in olfaction II: time course of recovery from adaptation in lobster chemoreceptor cells. *J. Neurophysiol.* **76**, 1340-1343.

Gomez, G. and Atema, J. (1996b). Temporal resolution in olfaction: stimulus integration time of lobster chemoreceptor cells. *J. Exp. Biol.* **199**, 1771-1779.

Gomez, G., Voigt, R. and Atema, J. (1994a). Frequency filter properties of lobster chemoreceptor cells determined with high-resolution stimulus measurement. *J. Comp. Physiol. A* **174**, 803-811.

Gomez, G., Voigt, R. and Atema, J. (1994b). Tuning properties of chemoreceptor cells of the American lobster: temporal filters. In *Olfaction and Taste*, vol. XI (ed. K. Kurihara, N. Suzuki and H. Ogawa), pp. 788-789. Tokyo: Springer-Verlag.

Gomez, G., Voigt, R. and Atema, J. (1999). Temporal resolution in olfaction III: flicker fusion and concentration-dependent synchronization with stimulus pulse trains of antennular chemoreceptor cells in the American lobster. *J. Comp. Physiol. A* **185**, 427-436.

Grünert, U. and Ache, B. (1988). Ultrastructure of the aesthetasc (olfactory) sensilla of the spiny lobster, *Panulirus argus*. *Cell Tissue Res.* **251**, 95-103.

Halpern, M. and Kubie, J. L. (1980). Chemical access to the vomeronasal organs of garter snakes. *Physiol. Behav.* **24**, 367-371.

Hansen, B. and Tiselius, P. (1992). Flow through the feeding structures of suspension feeding zooplankton: a physical model approach. *J. Plankton Res.* **14**, 821-834.

Holthuis, L. B. (1991). Marine lobsters of the world. In *FAO Species Catalog*, vol. 13, pp. 292. Rome: Food and Agriculture Organization of the United Nations.

Hunter, E. (1999). Biology of the European spiny lobster, *Palinurus elephas* (Fabricius, 1787) (Decapoda, Palinuridea). *Crustaceana* **72**, 545-565.

Kanciruk, P. (1980). Ecology of juvenile and adult Palinuridae (spiny lobsters). In *The Biology and Management of Lobsters*, vol. 2 (ed. J. S. Cobb and B. F. Phillips), pp. 59-96. New York: Academic Press.

Koehl, M. A. R. (1993). Hairy little legs: feeding, smelling, and swimming at low Reynolds number. *Contemp. Math.* **141**, 33-64.

Koehl, M. A. R. (1995). Fluid flow through hair-bearing appendages: feeding, smelling and swimming at low and intermediate Reynolds numbers. *Soc. Exp. Biol. Symp.* **49**, 157-182.

Koehl, M. A. R. (1996). Small-scale fluid dynamics of olfactory antennae. *Mar. Fresh. Behav. Physiol.* **27**, 127-141.

Koehl, M. A. R. (2000). Fluid dynamics of animal appendages that capture molecules: arthropod olfactory antennae. In *Computational Modeling in Biological Fluid Dynamics*, vol. 124 (ed. L. J. Fauci and S. Gueron), pp. 97-116. New York: Springer-Verlag.

Koehl, M. A. R., Koseff, J. R., Crimaldi, J. P., McCay, M. G., Cooper, T., Wiley, M. B. and Moore, P. A. (2001). Lobster sniffing: antennule design and hydrodynamic filtering of information in an odor plume. *Science* **294**, 1948-1951.

Kux, J., Zeiske, E. and Osawa, Y. (1988). Laser doppler velocimetry measurement in the model flow of a fish olfactory organ. *Chem. Senses* **13**, 257-265.

Laverack, M. S. (1964). The antennular sense organs of *Panulirus argus*. *Comp. Biochem. Physiol.* **13**, 301-321.

Laverack, M. S. (1985). The diversity of chemoreceptors. In *Sensory Biology*

of Aquatic Animals (ed. J. Atema, R. R. Fay, A. N. Popper and W. N. Tavolga), pp. 287-312. New York: Springer-Verlag.

Loudon, C., Best, B. A. and Koehl, M. A. R. (1994). When does motion relative to neighboring surfaces alter the flow through arrays of hairs? *J. Exp. Biol.* **193**, 233-254.

Loudon, C. and Koehl, M. A. R. (2000). Sniffing by a silkworm moth: wing fanning enhances air penetration through and pheromone interception by antennae. *J. Exp. Biol.* **203**, 2977-2990.

Lozano-Alvarez, E. and Biornes-Fourzan, P. (2001). Den choice and occupation patterns of shelters by two sympatric lobster species, *Panulirus argus* and *Panulirus guttatus*, under experimental conditions. *Mar. Fresh. Res.* **52**, 1145-1155.

MacDiarmid, A. B., Hickey, B. and Maller, R. A. (1991). Daily movement patterns of the spiny lobsters *Jasus edwarsii* (Hutton) on a shallow reef in northern New Zealand. *J. Exp. Mar. Biol. Ecol.* **147**, 185-205.

McWilliam, P. S. (1995). Evolution of the phyllosoma and puerulus phases of the spiny lobster genus *Panulirus* White. *J. Crust. Biol.* **15**, 542-557.

Mead, K. S., Koehl, M. A. R. and O'Donnell, M. J. (1999). Stomatopod sniffing: the scaling of chemosensory sensillae and flicking behavior with body size. *J. Exp. Mar. Biol. Ecol.* **241**, 235-261.

Moore, P. and Atema, J. (1988). A model of a temporal filter in chemoreception to extract directional information from a turbulent odor plume. *Biol. Bull.* **174**, 353-363.

Moore, P. A. and Atema, J. (1991). Spatial information in the three-dimensional fine structure of an aquatic odor plume. *Biol. Bull.* **181**, 408-418.

Moore, P. A., Atema, J. and Gerhardt, G. A. (1991a). Fluid dynamics and microscale chemical movement in the chemosensory appendages of the lobster, *Homarus americanus*. *Chem. Senses* **16**, 663-674.

Moore, P. A. and Grills, J. L. (1999). Chemical orientation to food by the crayfish *Orconectes rusticus*: influence of hydrodynamics. *Anim. Behav.* **58**, 953-963.

Moore, P. A., Scholz, N. and Atema, J. (1991b). Chemical orientation of lobsters, *Homarus americanus*, in turbulent odor plumes. *J. Chem. Ecol.* **17**, 1293-1307.

Oh, J. W. and Dunham, D. W. (1991). Chemical detection of conspecifics in the crayfish *Procambarus clarkii*: role of antennules. *J. Chem. Ecol.* **17**, 161-166.

Patek, S. (2001). Signal producing morphology and the evolution of palinurid lobster communication. Dissertation in Biology, pp. 127. Durham: Duke University.

Phillips, B. F., Cobb, J. S. and George, R. W. (1980). General biology. In *The Biology and Management of Lobsters: Physiology and Behavior*, vol. 1 (ed. J. S. Cobb and B. F. Phillips), pp. 1-82. New York: Academic Press.

Ptacek, M. B., Sarver, S. K., Childress, M. J. and Herrnkind, W. F. (2001). Molecular phylogeny of the spiny lobster genus *Panulirus* (Decapoda: Palinuridae). *Mar. Fresh. Res.* **52**, 1037-1047.

Ratchford, S. G. and Eggleston, D. B. (1998). Size- and scale-dependent chemical attraction contribute to an ontogenetic shift in sociality. *Anim. Behav.* **56**, 1027-1034.

Reeder, P. B. and Ache, B. W. (1980). Chemotaxis in the Florida spiny lobster, *Panulirus argus*. *Anim. Behav.* **28**, 831-839.

Schmiedel-Jakob, I., Anderson, P. A. V. and Ache, B. W. (1989). Whole cell recording from lobster olfactory receptor cells: responses to current and odor stimulation. *J. Neurophysiol.* **61**, 994-1000.

Schmitt, B. C. and Ache, B. W. (1979). Olfaction: responses of a decapod crustacean are enhanced by flicking. *Science* **205**, 204-206.

Sharp, W. C., Hunt, J. H. and Lyons, W. G. (1997). Life history of the spotted spiny lobster, *Panulirus guttatus*, an obligate reef-dweller. *Mar. Fresh. Res.* **48**, 687-698.

Snow, P. J. (1973). The antennular activities of the hermit crab, *Pagurus alaskensis* (Benedict). *J. Exp. Biol.* **58**, 745-765.

Sokal, R. R. and Rohlf, F. J. (1981). *Biometry*. New York: Freeman.

Steullet, P., Dudar, O., Flavus, T., Zhou, M. and Derby, C. D. (2001). Selective ablation of antennular sensilla on the Caribbean spiny lobster *Panulirus argus* suggests that dual antennular chemosensory pathways mediate odorant activation of searching and localization of food. *J. Exp. Biol.* **204**, 4259-4269.

Steullet, P., Krutzfeldt, D. R., Hamidani, G., Flavus, T., Ngo, V. and Derby, C. D. (2002). Dual antennular chemosensory pathways mediate odor-associative learning and odor discrimination in the Caribbean spiny lobster *Panulirus argus*. *J. Exp. Biol.* **205**, 851-867.

Sverdrup, H. U., Johnson, N. W. and Flemming, R. H. (1942). *The Oceans: Their Physics, Chemistry, and General Biology*. New York: Prentice-Hall Inc.

Trapido-Rosenthal, H. G., Carr, W. E. S. and Gleeson, R. A. (1987). Biochemistry of an olfactory purinergic system: dephosphorylation of excitatory nucleotides and uptake of adenosine. *J. Neurochem.* **49**, 1174-1182.

Vogel, S. (1994). *Life in Moving Fluids*. Princeton: Princeton University Press.

Weissburg, M. J. (2000). The fluid dynamical context of chemosensory behavior. *Biol. Bull.* **198**, 188-202.

Weissburg, M. J. and Zimmer-Faust, R. K. (1993). Life and death in moving fluids: hydrodynamic effects on chemosensory-mediated predation. *Ecology* **74**, 1428-1443.

Weissburg, M. J. and Zimmer-Faust, R. K. (1994). Odor plumes and how blue crabs use them in finding prey. *J. Exp. Biol.* **197**, 349-375.

Winter, D. A. (1990). *Biomechanics and Motor Control of Human Movement*. New York: John Wiley & Sons, Inc.

Zar, J. H. (1999). *Biostatistical Analysis*. New Jersey: Prentice-Hall.

Zimmer-Faust, R. K. and Case, J. F. (1983). A proposed dual role of odor in foraging by the California spiny lobster, *Panulirus interruptus* (Randall). *Biol. Bull.* **164**, 341-353.

Zimmer-Faust, R. K., Finelli, C. M., Pentcheff, N. D. and Wethey, D. S. (1995). Odor plumes and animal navigation in turbulent water flow: a field study. *Biol. Bull.* **188**, 111-116.

Zimmer-Faust, R. K., Tyre, J. E. and Case, J. F. (1985). Chemical attraction causing aggregation in the spiny lobster, *Panulirus interruptus* and its probable ecological significance. *Biol. Bull.* **169**, 106-118.